Chem. Soc. Rev., 1986, **15**, 141—165

Polyelectrodes: The Behaviour and Applications of Mixed Redox Systems

By Michael Spiro*
DEPARTMENT OF CHEMISTRY, IMPERIAL COLLEGE OF SCIENCE AND TECHNOLOGY, LONDON SW7 2AY

1 Introduction

Physical chemistry textbooks deal only with the behaviour of single redox couples. In real life, on the other hand, one often encounters two (or more) couples present together. Indeed, such situations form the basis of major industrial processes like the extraction of minerals from ores, electroless plating, and photographic development. Mixed redox systems are also at the root of the hugely expensive problem of metal corrosion. All these chemical phenomena can be satisfactorily explained by a simple additivity principle, and it is the main purpose of this review to show the many applications of such an approach.

2 Two Couples in Equilibrium

Let us take first a single redox couple like Fe^{3+}/Fe^{2+} or, in general, Ox/Red where

$$\mathrm{Ox} + ne^- \rightleftharpoons \mathrm{Red} \tag{1}$$

At equilibrium at an electrode, this couple will set up a potential E_{equil} (w.r.t. a standard hydrogen electrode) that obeys the well-known Nernst equation

$$E_{\mathrm{equil}} = E^{\ominus} + \frac{RT}{nF}\ln\frac{\{\mathrm{Ox}\}}{\{\mathrm{Red}\}} \tag{2}$$

where $E^{\ominus}$ is the standard potential of the couple, R is the gas constant, T the absolute temperature, F the Faraday constant, and where the curly brackets denote activities. Most electrochemical measurements are carried out in the presence of a supporting electrolyte like 1 mol dm^{-3} H_2SO_4 to prevent hydrolysis, keep the ratios of complexed species constant, and maintain the ionic strength at a given high value. The activity coefficients of the ions (y) are then approximately constant also, and equation 2 can be rewritten in terms of concentrations (square brackets):

$$E_{\mathrm{equil}} = E^{0} + \frac{RT}{nF}\ln\frac{[\mathrm{Ox}]}{[\mathrm{Red}]} \tag{3}$$

where the formal potential E^0 in this medium is given by

---

* This review is based in part upon a Keynote Lecture given at the H. N. Parton Symposium of the Golden Jubilee Conference of the New Zealand Institute of Chemistry in Auckland in August 1981 and on another Keynote Lecture given at the Electrochemistry Symposium of the 7th National Convention of the Royal Australian Chemical Institute in Canberra in August 1982.

$$E^0 = E^{\ominus} + \frac{RT}{nF}\ln\frac{y_{\mathrm{Ox}}}{y_{\mathrm{Red}}} \tag{4}$$

Equation 3 is much more practical than equation 2 for many purposes, and the formal potentials for common couples in standard media have been listed.[1]

Consider now the situation where two couples are simultaneously present and at equilibrium with each other. An example is a solution of 1 mol $\mathrm{dm^{-3}}$ H_2SO_4 containing $\mathrm{Fe^{III}}$ and $\mathrm{Fe^{II}}$ ions as well as $\mathrm{Ce^{IV}}$ and $\mathrm{Ce^{III}}$, with a platinum electrode and a reference electrode dipping into it. Since the reaction

$$\mathrm{Ce^{IV}} + \mathrm{Fe^{II}} \rightleftharpoons \mathrm{Ce^{III}} + \mathrm{Fe^{III}} \tag{5}$$

is very fast, the whole system rapidly comes to equilibrium. The potential on the platinum electrode is then given by the two Nernst equations:

$$E_{\mathrm{equil}} = E^0_{\mathrm{Fe^{III/II}}} + \frac{RT}{F}\ln\frac{[\mathrm{Fe^{III}}]}{[\mathrm{Fe^{II}}]} \tag{6a}$$

$$= E^0_{\mathrm{Ce^{IV/III}}} + \frac{RT}{F}\ln\frac{[\mathrm{Ce^{IV}}]}{[\mathrm{Ce^{III}}]} \tag{6b}$$

One can therefore calculate the potential using either couple provided the equilibrium concentrations are employed. This kind of calculation is familiar to anyone who carries out potentiometric titrations since the system is in equilibrium at every point along the titration curve. If a solution of $\mathrm{Fe^{II}}$ in a beaker is titrated with a $\mathrm{Ce^{IV}}$ solution in a burette, it is convenient to use equation 6a before the equivalence point and equation 6b after it.[2]

Let us return to the single redox couple (1). So far it has been assumed that its equilibrium potential E_{equil} is set up rapidly at the electrode surface, but this is true only for fairly 'electrochemically reversible' couples like $\mathrm{Fe^{III}/Fe^{II}}$. If the rates of interconversion $\mathrm{Ox} + ne^- \longrightarrow \mathrm{Red}$ and $\mathrm{Red} \longrightarrow \mathrm{Ox} + ne^-$ are slow, the couples are 'electrochemically irreversible'. These interconversion rates can be expressed in mol $\mathrm{m^{-2}\ s^{-1}}$ or, by introducing Faraday's law to convert moles into coulombs, in the electrochemical units A $\mathrm{m^{-2}}$. At equilibrium, where the interconversion rates are equal, these current densities are termed exchange current densities, i_0. Truly reversible couples possess i_0 values exceeding 1 A $\mathrm{cm^{-2}}$ whereas those with i_0 below 1 μA $\mathrm{cm^{-2}}$ are very irreversible. Couples in the latter category do not adequately 'poise' the potential of an electrode; the potential slowly drifts and even if it appears to reach a steady value it usually does not obey the Nernst equation because the electrode is influenced by traces of impurities (see Section 5). How then can one determine the standard or formal potential of such a couple? A good example is provided by the chemistry of neptunium. When enough material (a few milligrams) of this new element had been isolated in the 1940s, experiments were carried out to

---

[1] R. G. Bates, 'Electrode Potentials', in 'Treatise on Analytical Chemistry', ed. I. M. Kolthoff and P. J. Elving, Wiley-Interscience, New York, 1978, 2nd Edn., Part I, Vol. 1, Chapt. 13 (see pp. 808—809); A. J. Bard, R. Parsons, and J. Jordan, 'Standard Potentials in Aqueous Solution', Dekker, New York, 1985.

[2] E. Bishop, 'Theory and Principles of Inorganic Titrimetric Analysis', in 'Comprehensive Analytical Chemistry', ed. C. L. Wilson and D. W. Wilson, Elsevier, Amsterdam, 1960, Vol. 1B, Chapt. VII (see pp. 134—135).

characterize its various oxidation states in solution.[3] The Np^{V}/Np^{IV} couple, however, behaved irreversibly and its standard potential could not be measured directly. The problem was solved by introducing a second couple that did behave reversibly, Fe^{III}/Fe^{II}. The chemical reaction

$$Np^{V} + Fe^{II} \rightleftharpoons Np^{IV} + Fe^{III} \tag{7}$$

was found to reach equilibrium after about 80 min, and the extent of the reaction was determined spectrophotometrically. A platinum electrode immersed in the equilibrium mixture now registered a steady and reproducible potential because it was poised by the Fe^{III}/Fe^{II} couple. Since the system was in overall equilibrium, this potential was also equal to the Nernst potential of the neptunium couple

$$E_{\text{equil}} = E^{0}_{\text{Np}^{\text{V/IV}}} + \frac{RT}{F}\ln\frac{[\text{Np}^{\text{V}}]}{[\text{Np}^{\text{IV}}]} \tag{8}$$

from which its E^0 could be calculated. In this situation the iron couple acted as a 'potential mediator'. A successful mediator must clearly fulfil certain criteria: it must itself poise the potential well, it must react reasonably rapidly with the couple in question, and its formal potential should be near to that of the couple being mediated. The basic concept of a potential mediator dates back to the beginning of this century; in 1907, for example, the I_2/I^- couple was used to obtain the standard potential of the electrochemically sluggish As^{V}/As^{III} couple.[4] In recent years the idea has been fruitfully applied to the determination of standard potentials of organic[5] and especially of biological redox couples.[6]

3 Couples not in Equilibrium: the Kinetic Factor

The preceding section has dealt with some carefully selected mixed redox systems that rapidly come to equilibrium with each other and with the electrode. Relatively few mixed systems do. This is partly because homogeneous redox reactions are rarely fast, and partly because only a minority of couples are electrochemically reversible. We must therefore look at the kinetic aspects, beginning with those of a single couple.

Consider a vessel containing the Ox/Red electrode system, as well as a counter electrode to allow current to flow and a reference electrode to monitor the potential.[7,8] Let us impress on the test electrode a potential E that differs from the Nernst potential E_{equil}. This extra or over-potential η defined by

---

[3] J. C. Hindman, L. B. Magnusson, and T. J. LaChapelle, *J. Am. Chem. Soc.*, 1949, **71**, 687.

[4] L. Loimaranta, *Z. Elektrochem.*, 1907, **13**, 33; R. Luther, *ibid.*, 1907, **13**, 289.

[5] W. M. Clark, 'Oxidation–Reduction Potentials of Organic Systems', Williams and Wilkins, Baltimore, 1960.

[6] E. Steckhan and T. Kuwana, *Ber. Bunsenges.*, 1974, **78**, 253.

[7] A. J. Bard and L. R. Faulkner, 'Electrochemical Methods', Wiley, New York, 1980, Chapt. 1, 3. Note that this book employs the now superseded convention of taking cathodic currents as positive.

[8] R. Greef, R. Peat, L. M. Peter, D. Pletcher, and J. Robinson, 'Instrumental Methods in Electrochemistry', Ellis Horwood, Chichester, 1985, Chapt. 1, 3, 4, 11.

$$\eta = E - E_{\text{equil}} \tag{9}$$

alters the activation energy of the electrode reactions by a proportionate amount and thus affects their rates. If η is positive (an anodic overpotential), the Red $\longrightarrow$ Ox + ne^- process speeds up and the Ox + ne^- $\longrightarrow$ Red process slows down, and the reverse is true if η is negative (a cathodic overpotential). Since the current that flows across the test electrode/solution interface is the difference between the anodic (oxidation) and the cathodic (reduction) currents, we obtain the Butler–Volmer equation[8] for the net current density i

$$i = i_{\text{anod}} - i_{\text{cath}} = i_0\left[\exp\left(\frac{\alpha_{\text{anod}}nF\eta}{RT}\right) - \exp\left(\frac{-\alpha_{\text{cath}}nF\eta}{RT}\right)\right] \tag{10}$$

Here α_{anod} and α_{cath} are the anodic and cathodic transfer coefficients which are often around $\frac{1}{2}$, and for simple electron-transfer reactions

$$\alpha_{\text{anod}} + \alpha_{\text{cath}} = 1 \tag{11}$$

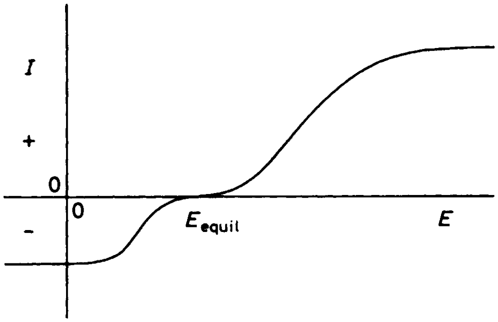

Figure 1 *Schematic current–potential curve for an irreversible redox couple*

Figure 1 shows a typical current–potential curve for an irreversible redox couple. At low overpotentials the current density rises linearly with potential because the two exponential terms in equation (10) almost cancel each other out, leaving behind

$$i = i_0 nF\eta(\alpha_{\text{anod}} + \alpha_{\text{cath}})/RT \tag{12}$$

Notice that the slope $\mathrm{d}i/\mathrm{d}\eta$ is proportional to i_0. The i–E curve is therefore very steep near the equilibrium potential for fairly reversible couples and almost horizontal for highly irreversible ones. At sufficiently large overpotentials ($|\eta| >$ *ca.* 0.1 V), one of the two exponential terms in (10) becomes negligibly small compared with the other. This gives rise to the two Tafel equations

$$\ln\left(\frac{\quad}{\quad}\right) = \frac{\alpha_{\text{anod}} nF\eta}{RT} \quad \text{(anodic region)} \tag{13a}$$

$$\ln\left(\frac{-i}{i_0}\right) = \frac{-\alpha_{\text{cath}} nF\eta}{RT} \quad \text{(cathodic region)} \tag{13b}$$

The signs show that anodic currents are taken as positive and cathodic ones as negative, as proposed by IUPAC.[9]

When the overpotential is higher still, the electron transfer across the interface is so fast that the rate-limiting step becomes the supply of Red (on the anodic side) or of Ox (on the cathodic side) to the electrode surface. In order to reach the surface the electroactive species j must diffuse through the adjacent diffusion layer (or Nernst film) of thickness δ. It then follows from Fick's first law of diffusion and Faraday's law that the maximum or limiting current density is[7,8]

$$i_{\text{lim}} = \frac{nFD_j c_j}{\delta} \tag{14}$$

where c_j is the bulk concentration of j and D_j is its trace diffusion coefficient in the supporting electrolyte medium. This equation explains the existence of the horizontal plateaux in Figure 1. The thickness δ is essentially a function of the hydrodynamic flow conditions around the electrode: faster stirring decreases δ and so increases i_{lim}. Under given stirring conditions the limiting current is proportional to the bulk concentration of the electroactive species, an important result for polarography and other electroanalytical techniques.

4 Two Couples not in Equilibrium

From now on we shall deal with the situation that arises when two (or more) couples are present together but are *not* in equilibrium with each other. A system of this kind is often called a 'polyelectrode'.[10,11] Its treatment is greatly simplified by an additivity principle that was clearly expounded, tested, and popularized by Wagner and Traud in 1938[12] and often attributed to them although the idea was not entirely new at the time they wrote their paper. The principle is based on the assumption that the couples present act independently of each other. Thus at any given potential, each couple is assumed to exhibit its own individual current, and the current observed in the laboratory is their algebraic sum. There will be one potential at which the net observed current is zero, the point at which the anodic current due to one couple exactly balances the cathodic current of the other couple. This is shown diagrammatically in Figure 2. The potential of zero net current is

---

[9] R. Parsons, *Pure Appl. Chem.*, 1974, **37**, 512.

[10] J. O'M. Bockris, 'Electrode Kinetics', in 'Modern Aspects of Electrochemistry', ed. J. O'M. Bockris and B. E. Conway, Butterworths, London, 1954, Chapt. 4, Section X.

[11] P. Van Rysselberghe, *Electrochim. Acta*, 1964, **9**, 1343.

[12] C. Wagner and W. Traud, *Z. Elektrochem.*, 1938, **44**, 391.

normally called the mixed potential,[10] a term which implies a mixing of voltages. In fact the potential is a singular one and it is therefore preferable to call it the mixture potential, E_{mix}. It is E_{mix} that one measures with a digital voltmeter or potentiometer when a mixture of couples is present together at an electrode.

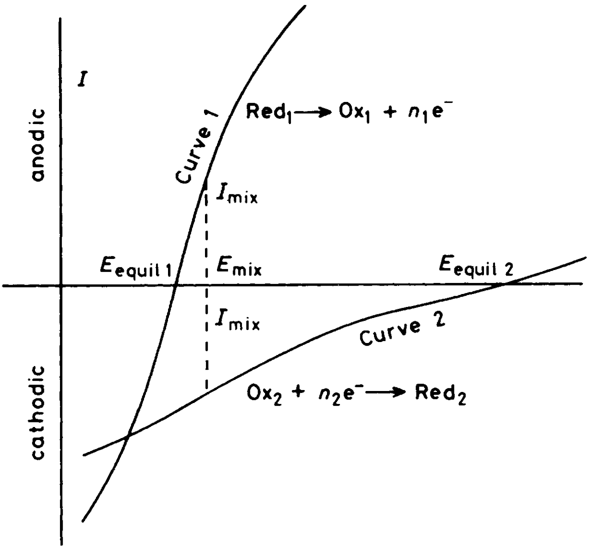

Figure 2 *Schematic diagram showing the effect of two couples present together but not in equilibrium with each other*

The currents that balance out at E_{mix} are called mixture currents and given the symbol I_{mix}. These two equal mixture currents represent not only the rates of the two half-reactions $Red_1 \longrightarrow Ox_1 + n_1e^-$ and $Ox_2 + n_2e^- \longrightarrow Red_2$ but also the rate (V) of the overall redox reaction that takes place between the couples at E_{mix}. If n electrons have cancelled out when adding up the two half-reactions, then by Faraday's law

$$V = I_{mix}/nF \tag{15}$$

If the corresponding current density i_{mix} is used instead, we obtain the surface reaction rate v (in mol m^{-2} s^{-1}):

$$v = V/A = i_{mix}/nF \tag{16}$$

where A is the surface area.

The additivity principle has been tested experimentally by several workers[12–21] and, in the great majority of cases, was found to hold within the uncertainties of measurement. Some recently discovered exceptions will be mentioned later in Section 10. Another series of publications[10,12,20,22–33] has developed the theory of mixture potentials and mixture currents and the way in which they depend on the type of couple, the concentrations of the electroactive species, the stirring conditions, time, and other variables. The present review, however, will not focus on these mathematical expositions but aims instead to illustrate the application and utility of the underlying concept in several areas of chemistry.

5 Electrode Poisoning

Section 2 referred to the difficulty of measuring the equilibrium potential of an electrochemically irreversible couple like Np^V/Np^{IV}. If the exchange current density i_0 of such a couple is small one might expect to have to wait a long time before the correct Nernst potential is established, but in practice this is never attained at all. Why not? The reason is that all solutions contain traces of impurities, and some of these are the components of other couples. It is then E_{mix} of the whole system that is measured rather than the equilibrium potential of the original couple. Two classical examples may be cited. The first is the poisoning of the hydrogen electrode by traces of oxygen or other oxidants like Fe^{3+}, a situation investigated by Wagner and Traud.[12] Although the H^+/H_2 couple possesses a fairly high exchange current density (*cf.* curve 1 in Figure 2) and the O_2/H_2O couple one as low as 10^{-10} A cm^{-2} (*cf.* curve 2), the two equilibrium potentials are so far apart that E_{mix} is significantly higher than E_{equil} for the hydrogen couple. The more oxygen is present the steeper is curve 2 and the more positive does E_{mix} become. The second example concerns the oxygen couple itself:

$$O_2(g) + 4H^+ + 4e^- \rightleftharpoons 2H_2O \qquad (17)$$

Attempts to determine its potential by bubbling oxygen around a platinum electrode in an acid solution always failed, the measured potential being some 0.4 V lower than the value calculated from thermodynamic data. Because the oxygen

---

[13] I. M. Kolthoff and C. S. Miller, *J. Am. Chem. Soc.*, 1940, **62**, 2171.
[14] J. V. Petrocelli, *J. Electrochem. Soc.*, 1950, **97**, 10.
[15] A. C. Makrides, *J. Electrochem. Soc.*, 1960, **107**, 869.
[16] M. Paunovic, *Plating*, 1968, 1161.
[17] M. Spiro and P. W. Griffin, *Chem. Comm.*, 1969, 262.
[18] R. Woods, *J. Catal.*, 1970, **16**, 267.
[19] Z. Takehara, *Electrochim. Acta*, 1970, **15**, 999.
[20] J. M. Herbelin, T. N. Andersen, and H. Eyring, *Electrochim. Acta*, 1970, **15**, 1455.
[21] M. Spiro and P. L. Freund, *J. Electroanal. Chem.*, 1983, **144**, 293.
[22] M. Stern and A. L. Geary, *J. Electrochem. Soc.*, 1957, **104**, 56.
[23] F. A. Posey, *J. Electrochem. Soc.*, 1959, **106**, 571.
[24] P. J. Gellings, *Ber. Bunsenges.*, 1963, **67**, 167.
[25] A. Tockstein, *Coll. Czech. Chem. Commun.*, 1965, **30**, 3621; 1966, **31**, 2466.
[26] A. Tockstein and M. Matusek, *Coll. Czech. Chem. Commun.*, 1967, **32**, 1309. 3089.
[27] C. Wagner, *Electrochim. Acta*, 1970, **15**, 987.
[28] S. Barnartt, *Electrochim. Acta*, 1970, **15**, 1313.
[29] T. Kodera, H. Kita, and M. Honda, *Electrochim. Acta*, 1972, **17**, 1361.
[30] D. B. Matthews, *Aust. J. Chem.*, 1975, **28**, 243.
[31] M. Spiro, *J. Chem. Soc.. Faraday Trans. I*, 1979, **75**, 1507.
[32] G. P. Power and I. M. Ritchie, *Electrochim. Acta*, 1981, **26**, 1073.
[33] P. L. Freund and M. Spiro, *J. Chem. Soc.. Faraday Trans. I*, 1983, **79**, 481.

couple is so irreversible, tiny traces of electroactive impurities were able to exert an undue effect.[34] Not until Bockris and Huq[35] ultra-purified their solutions was it possible to obtain the correct Nernst potential by direct measurement.

Poisoning effects become more pronounced at low concentrations of the electroactive ions because exchange current densities are concentration dependent. For a simple couple like Fe^{3+}/Fe^{2+} the relationship is[7,8]

$$i_0 = Fk^{\ominus}[Fe^{3+}]^{\alpha_{anod}}[Fe^{2+}]^{\alpha_{cath}} \tag{18}$$

where $k^{\ominus}$ is the standard rate constant. Thus when one or both components of the couple are present in very low concentration its exchange current density is small and, by equation 12, its current–potential curve becomes flatter. An impurity couple will then move E_{mix} further away from E_{equil}. This accounts for the many reports of deviations from the Nernst equation when the concentration of one component (*e.g.*, Br_2 in the Br_2/Br^- couple[36]) sinks below *ca.* 10^{-6} mol dm^{-3}. An interesting example occurs at the equivalence point of the titration between Ag^+ and I^-. Here the concentrations of both electroactive ions are extremely small and so dissolved oxygen, either alone or through oxidation of iodide to iodine, can largely control the potential.[37] Sometimes oxygen can even be generated by the system itself, as in solutions that contain only the oxidant form (*e.g.*, Ce^{4+}) of a couple. The initial potential is then so high that some solvent is oxidized and the products set up a mixture potential.[38] Undoubtedly mixture potentials are the explanation for certain weird e.m.f. observations that are scattered through the literature.

6 Dissolution of Metals

Early this century Van Name and Hill[39] found that disks of many metals (Fe, Co, Ni, Cu, Ag, Zn, Cd, Hg) dissolved at essentially the same rate in a given solution of iodine in KI, and that the rate increased with stirring speed. The same phenomenon occurred when different oxidizing agents were employed: thus ferric alum solutions in concentrated sulphuric acid attacked disks of Fe, Ni, Cu, Cd, and Sn at an equal rate, with only silver dissolving more slowly. Such results are surprising to a chemist who would expect each metal to react at its own individual rate. A simple explanation was subsequently given by Hoar[40] in terms of current–potential curves. As Figure 3 shows, the anodic dissolution curve for each metal

$$M(c) \longrightarrow M^{2+} + 2e^- \tag{19}$$

is indeed peculiar to itself. However, over the potential range in question the Fe^{3+}

---

[34] T. P. Hoar, *Proc. Roy. Soc. A*, 1933, **142**, 628.

[35] J. O'M. Bockris and A. K. M. S. Huq, *Proc. Roy. Soc. A*, 1956, **237**, 277.

[36] W. C. Purdy, E. A. Burns, and L. B. Rogers, *Anal. Chem.*, 1955, **27**, 1988.

[37] R. B. Hanselman, G. H. Schade Jr., and L. B. Rogers, *Anal. Chem.*, 1960, **32**, 761.

[38] F. Verbeek and J. Eeckhaut, *Bull. Soc. Chim. Belg.*, 1958, **67**, 64, 204; 1959, **68**, 303.

[39] R. G. Van Name and D. U. Hill, *Amer. J. Sci.*, 1916, **42**, 301.

[40] T. P. Hoar, 'The Anodic Behaviour of Metals', in J. O'M. Bockris, ed., 'Modern Aspects of Electrochemistry', Butterworths, London, 1959, No. 2, Chapt. 4, Section VI.

reduction curve exhibits a long limiting current plateau. The mixture potential thus varies from metal to metal but the mixture currents are all the same. It is these mixture currents that, by equation 15 with $n = 2$, express the rates (in mol s^{-1}) of the overall reactions

$$M(c) + 2Fe^{3+} \longrightarrow M^{2+} + 2Fe^{2+} \qquad (20)$$

Salzberg and King[41] found that the rates were proportional to the Fe^{III} concentration and increased with increasing stirring speed. These findings are easily explained by the fact that the mixture currents are equal to the Fe^{3+} limiting diffusion current which, by equation 14, is proportional to $[Fe^{3+}]/\delta$. It is also clear from Figure 3 why silver was the only metal to dissolve more slowly in the Fe^{III} solutions. Its equilibrium potential is quite close to that of the Fe^{3+}/Fe^{2+} couple and the I_{mix} value is thus considerably smaller. This peculiarity of silver should disappear if an oxidizing agent of much higher formal potential is employed and indeed, when Ce^{4+} was substituted for Fe^{3+}, Salzberg *et al.*[42] found that copper and silver were attacked at the same rate, both reactions being diffusion controlled. The electrochemical interpretation of metal dissolution has therefore made sense of a large number of different observations.

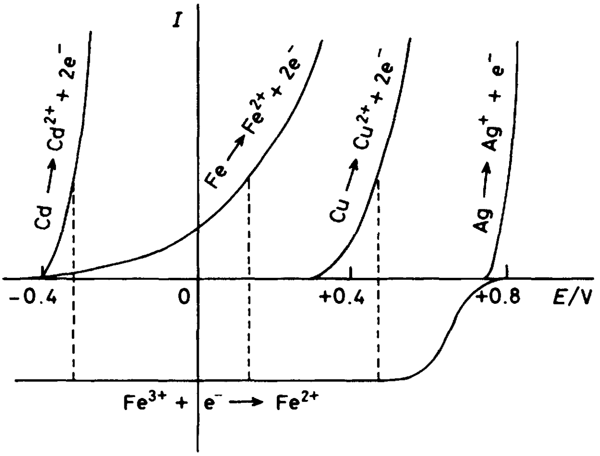

Figure 3 *Electrochemical interpretation of the kinetics of dissolution of various metals in acid solutions of iron*(III)

The mechanism by which reaction 20 proceeds is pictured in Figure 4. Because the corroding metal has adopted a potential E_{mix} that lies between the equilibrium potentials of the M^{2+}/M and the Fe^{3+}/Fe^{2+} couples, the metal can act simultaneously as an anode producing M^{2+} ions and as a cathode reducing Fe^{3+}

---

[41] H. W. Salzberg and C. V. King, *J. Electrochem. Soc.*, 1950, **97**, 290.

[42] H. W. Salzberg, H. Knoetgen, and A. M. Molless, *J. Electrochem. Soc.*, 1951, **98**, 31.

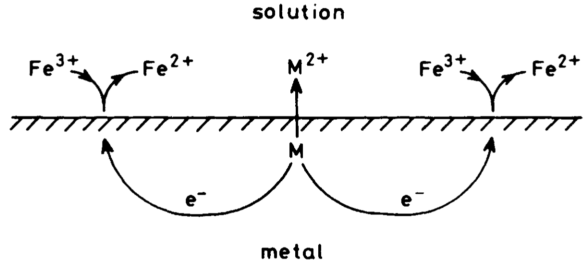

Figure 4 *Mechanistic picture of a metal corroding in iron*(III) *solutions*

ions to Fe^{2+}. At E_{mix} the flow of electrons through the metal resulting from M^{2+} formation exactly balances the flow required for the equivalent Fe^{3+} reduction: this flow therefore measures the rate of the overall reaction (20). It must be emphasized that no external potential has been imposed as from a battery – the electrochemical mechanism is set up by the system itself.

While other metal dissolutions and most types of reaction involving two couples operate by similar electrochemical mechanisms, the reaction kinetics may be quite different. The five main ways in which the rate can be controlled are sketched in Figure 5, and follow Hoar's classification.[40] Situation (a) arises when an electrochemically irreversible cathodic process is coupled with an electrochemically reversible anodic one; here I_{mix} and hence the overall rate are essentially determined by the energy barrier in the cathodic process. The converse is shown in (b). In (c) both couples exhibit roughly equal degrees of reversibility and there is joint control by the anodic and cathodic energy barriers. Reactions (a)—(c) are said to be activation controlled whereas (d) and (e) are transport controlled. Case (d) is the one we have already met in Figure 3: the mixture potential lies in the limiting current region of the cathodic process and the overall rate is controlled by the rate at which the cathodic reactant (*e.g.*, Fe^{3+}) arrives at the surface by diffusion and/or convection. The converse situation, pictured at (e), was recently encountered by Parker and his co-workers[43,44] in studying the extraction of copper from chalcopyrite, $CuFeS_2$. They found that the rates of leaching at 80 °C varied relatively little with a wide range of oxidants because the rate-determining step in each case was the slow transport of species through a metal-deficient polysulphide film formed on the surface of the mineral. The rate of copper extraction was therefore diffusion-controlled but unaffected by stirring the solution.

Processes controlled by diffusion through the liquid can be distinguished from activation-controlled processes by altering the hydrodynamic flow conditions. This can easily be done by using a flat circular disk of the solid, set in an inert former, and rotating it about a vertical axis (Figure 6) at a series of rotation speeds f. The resulting diffusion layer over the surface is then of uniform thickness δ given by[45]

[43] A. J. Parker, R. L. Paul, and G. P. Power, *Aust. J. Chem.*, 1981, **34**, 13.

[44] A. J. Parker, R. L. Paul, and G. P. Power, *J. Electroanal. Chem.*, 1981, **118**, 305.

[45] V. G. Levich, 'Physicochemical Hydrodynamics', Prentice-Hall, Englewood Cliffs, N.J., 1962, Section 11.

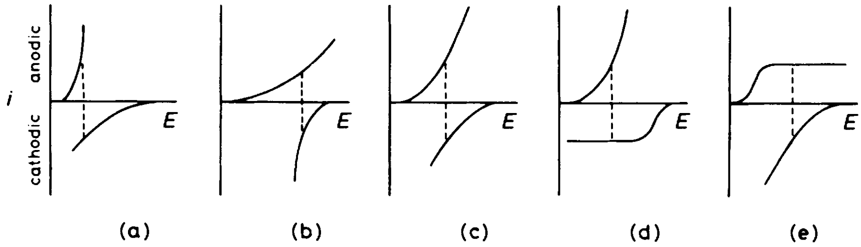

Figure 5 *Five major types of electrochemical control*

$$\delta = 0.643\, D_j^{1/3} \nu^{1/6} f^{-1/2} \quad (21)$$

where f is in Hz (s^{-1}), D_j is the trace diffusion coefficient of the electroactive species in question, and ν the kinematic viscosity of the solution (= viscosity/density). Combination of the Levich equation (21) with equations (14) and (16) shows that the rates of transport-controlled reactions will rise proportionately with $\sqrt{f}$. The rates of activation-controlled reactions, on the other hand, will be quite independent of the rotation speed. Power and Ritchie[32,46] have recently derived equations for the way in which E_{mix} depends upon rotation speed and reactant concentration in various types of metal dissolutions including cases (c), (d), and (e) of Figure 5 as well as for situations where coherent product layers are formed on the metal.

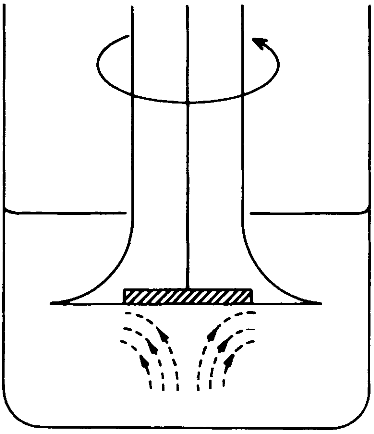

Figure 6 *Illustration of a solid (shown hatched) set into a rotating disk. The trumpet shape of the inert former keeps separate the flows above and below the disk (shown dotted)*

It should be made clear that such mechanistic studies are of considerable

---

[46] G. P. Power, W. P. Staunton, and I. M. Ritchie, *Electrochim. Acta*, 1982, **27**, 165.

practical importance to the mining industry. Metals are increasingly being extracted from their ores by 'wet' or hydrometallurgical processes[47] whose first step involves a coupled reaction with an oxidizing agent. Not only the metal itself but also the sulphide or oxide can be extracted in this way, as in the leaching of uranite (uranium dioxide) to form UO_2^{2+} in solution.[48] The chemical rates of leaching with various oxidizing agents were found to agree closely with those calculated from the anodic currents of the half reaction

$$UO_2(c) \longrightarrow UO_2^{2+} + 2e^- \tag{22}$$

at potentials equal to the E_{mix} values measured in the corresponding leaching experiments. Leaching rates could therefore be predicted from electrochemical data. The application of the additivity of current–potential curves in this example again illustrates its usefulness. Kinetic and mechanistic knowledge of this kind materially assist in the choice of oxidant and plant design so that mineral extractions can be carried out efficiently and economically.

So far it has been tacitly assumed that the whole of the surface is equally accessible to both couples or at least that the anode and cathode areas are the same. This is a reasonable proposition provided the surface sites are all of the same kind and provided also that the time taken by cathodic acts on any site is short compared with the period when the site is free to act anodically, and *vice versa*.[40] There is then little mutual interference between the anodic and cathodic processes. Several of the theoretical treatments in the literature have however taken the anodic and cathodic areas to be different. Situations certainly exist in which there are good physical reasons for dividing the surface into anodic and cathodic patches. Metal displacement or cementation reactions provide very clear examples. In these the oxidant is itself reduced to a metal and precipitates on the reacting surface, as in the reaction[49]

$$Fe(c) + Cu^{2+} \longrightarrow Fe^{2+} + Cu(c) \tag{23}$$

This particular process is used industrially to recover copper from dilute solutions by the addition of iron powder.[47] As the copper deposit increasingly encroaches upon the iron surface, the area A_{anod} available for anodic iron dissolution must decrease.[49] Quite generally, when the areas of the anodic and cathodic processes are not the same, the respective current densities i are related by the equation

$$i_{anod}A_{anod} = I_{anod} = -I_{cath} = -i_{cath}A_{cath} \tag{24}$$

since the anodic and cathodic mixture currents must be equal at E_{mix}. Equation 24 finds most frequent application in the study of corrosion.

---

[47] A. R. Burkin, 'The Chemistry of Hydrometallurgical Processes', Spon, London, 1966.

[48] M. J. Nicol, C. R. S. Needes, and N. P. Finkelstein, 'Electrochemical Model for the Leaching of Uranium Dioxide', in 'Leaching and Reduction in Hydrometallurgy', ed. A. R. Burkin, IMM, London, 1975, p. 1.

[49] G. P. Power and I. M. Ritchie, 'Metal Displacement Reactions', in 'Modern Aspects of Electrochemistry', eds. B. E. Conway and J. O'M. Bockris, Plenum, New York, 1975, Vol. 11, Chapt. 5.

7 Corrosion

Whereas metal leaching is a desirable process, the corrosion of metals is highly undesirable. Whole structures or manufacturing processes can collapse through the corrosion of a small vital part. Many billions of pounds are lost annually around the world through the cost of replacing corroded parts or on preventative treatment. Metals have long been known to corrode by an electrochemical mechanism[50–52] and the subject is conveniently treated by the superposition of current–potential curves. Indeed, the reaction investigated by Wagner and Traud[12] in their classical paper was the dissolution of zinc from zinc amalgam in hydrochloric acid. Let us therefore look more generally at metal corrosion in acid solution. Piontelli[53,54] has conveniently classified metals into three categories and the corresponding I–E curves are sketched in Figure 7. The metals in Figure 7(a) like Ag, Cd, Hg, Tl, Sn, and Pb are called 'normal': they are low melting with weak metal–metal bonds. The exchange current densities i_0 of the M^{n+}/M couples are consequently high (10^{-3}—10 A cm^{-2} in 1 mol dm^{-3} solutions of the metal ions) and the I–E curves steep. However, the i_0 values of the H^+/H_2 couple on these surfaces are low and its I–E curves slope very gently. Thus the mixture potential is always very close to the formal potential of the metal couple, as shown in the diagram. The current at E_{mix}, *i.e.* the corrosion rate, is therefore largely determined by the electrode kinetics of H^+ reduction on the metal surface. The contrary situation appears in Figure 7(b). The 'inert' or 'sluggish' metals whose behaviour is represented here, high-melting ones like Fe, Co, Ni, and other transition metals as well as noble metals such as Au, Rh, and Pt, possess strong metal–metal bonds and

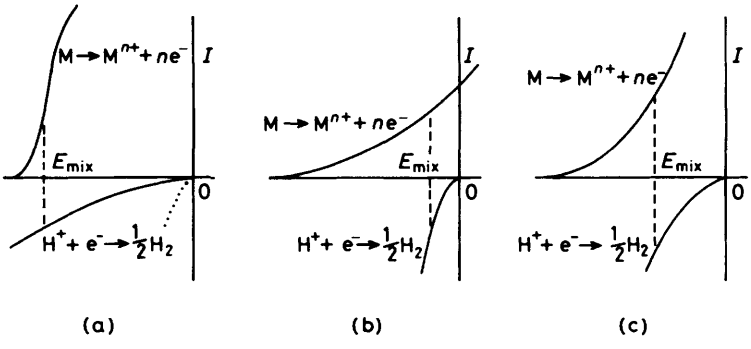

Figure 7 *Schematic representation of the corrosion in acid solution of three different types of metal according to Piontelli's classification:* (*a*) *'normal' metals.* (*b*) *'inert' metals,* (*c*) *'intermediate' metals*

---

[50] J. O'M. Bockris and A. K. N. Reddy, 'Modern Electrochemistry', Plenum, New York, 1970, Vol. 2.

[51] U. R. Evans, 'An Introduction to Metallic Corrosion', Edward Arnold, London, 3rd Edn., 1981.

[52] G. Wranglen, 'An Introduction to Corrosion and Protection of Metals', Chapman and Hall, London, 2nd Edn., 1985.

[53] R. Piontelli, *Chem. Ind.*, 1957, 1304.

[54] D. A. Vermilyea, 'Anodic Films', in 'Advances in Electrochemistry and Electrochemical Engineering', ed. P. Delahay, Interscience-Wiley, New York, 1963, Vol. 3, Chapt. 4 (see p. 222).

are oxidized only with difficulty. Thus the i_0 values of these M^{n+}/M couples are small (10^{-15}–10^{-8} A cm^{-2} in 1 mol dm^{-3} solutions) and large overpotentials are needed to produce appreciable currents (equation 13a). The H^+/H_2 couple, on the other hand, is electrochemically reversible on these metal surfaces and so the mixture potential is near the Nernst potential of the hydrogen electrode. The corrosion rate therefore depends mainly upon the anodic behaviour of the metal. Finally, Figure 7(c) depicts typical curves for 'intermediate' metals such as Cu, Sb, and Zn with i_0 values for M^{n+}/M in the range 10^{-8}—10^{-3} A cm^{-2} in 1 mol dm^{-3} solutions. It will be evident that Figures 7(a)—(c) represent examples of the general categories 5(a)—(c) that were discussed earlier.

Certain useful corollaries follow. If a relatively soft metal like zinc has on it impurity spots of an inert metal like iron (or better still, platinum), then the reduction of H^+ will take place exclusively on these latter spots with an I–E curve like the dotted one in Figure 7(a). The corrosion rate will thus be hugely increased. This explains why pure zinc is not readily attacked by acids while impure zinc dissolves with alacrity. Now let us turn this example round. If a piece of iron is in good electrical contact with a piece of zinc, H^+ reduction will occur only on the iron surface and the zinc alone will dissolve. This is made use of in protecting buried iron pipelines and oil platforms in the North Sea by attaching portions of zinc (or magnesium) which preferentially dissolve as 'sacrificial anodes'. The current density at the zinc surface will be quite high, as equation 24 shows, and from time to time the anode will need to be replaced. Another major method of protecting a pipeline or other metallic structure is to impress a cathodic potential on it: this is done by means of an external d.c. source and a graphite or stainless steel anode buried nearby. It is evident from Figure 7 that a metal held at its equilibrium potential cannot dissolve anodically although H^+ would be rapidly reduced at its surface by electrons flowing in from the external power supply.

Usually metals are not immersed in acid solutions and the cathodic process that partners their dissolution is then the reduction of oxygen (equation 17). In neutral solution the potential of the oxygen couple is 0.81 V, and it is electrochemically irreversible. The corrosion current at E_{mix} is therefore small unless the formal potential of the metal couple is sufficiently negative. This is the case for iron, the metal whose corrosion we most frequently want to avoid in practice. The standard potential of the Fe^{2+}/Fe couple is -0.44 V, and its Nernst potential is even smaller in the presence of the OH^- ions formed by the oxygen reduction. This important topic will now be illustrated with an Evans diagram.[55,51,52] Extensively employed by metallurgists, the Evans diagram is a modification of the type of current–potential curve favoured by electrochemists. The main differences are:

(i) In the Evans diagram potential is plotted on the vertical axis and current on the horizontal axis.

(ii) Anodic and cathodic currents are both taken as positive.

(iii) Currents are usually represented in the form of log (current). The plots are therefore linear in the Tafel regions although regretfully many corrosion scientists

---

[55] U. R. Evans, *J. Franklin Inst.*, 1929, **208**, 52.

draw straight E–log$I$ lines down to currents so small that the Tafel approximation (equation 13) of the Butler–Volmer equation (10) is no longer valid.

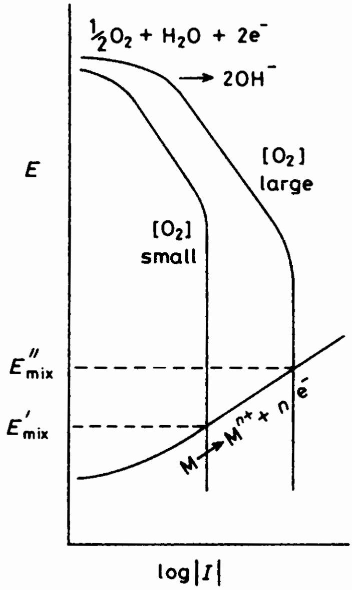

Figure 8 *Evans diagram showing the corrosion of a metal in solutions containing a low and a high concentration of oxygen*

Figure 8 is a typical Evans diagram for the corrosion of a metal like iron. The corrosion rate (the current) at E'_{mix} is smaller than at E''_{mix} where the oxygen concentration in solution is greater. The reaction is therefore under cathodic control and corresponds to diagram 5(d). Although Figure 8 describes what happens when the oxygen concentration is uniform over the whole surface, a rather different situation arises during differential aeration. Take an iron or steel specimen partially immersed in salt water. The section just below the waterline will be well aerated while further down into the water the oxygen concentration is less. The upper part of the metal therefore adopts a potential positive with respect to that on the lower part, and so electrons will flow upwards through the metal specimen. The top part of the metal now acts as a cathode and reduces oxygen while the bottom end of the metal becomes anodic and dissolves. The anodic and cathodic processes thus occur on different parts of the metal. Nature here operates in a way that appears contrary to common sense: that part of the metal most exposed to oxygen is actually protected from attack while the section furthest away, with limited access to the oxidant, corrodes. A particularly serious problem arises when the cathodic area is large and the anodic area small, as with a wet crack or crevice. Here, by equation 24, the anodic current density attains a high value and the bottom of the crevice corrodes rapidly, a phenomenon known as pitting corrosion. It would be unfair to end this section without pointing out that oxygen can also be an ally, protecting a metal surface from attack by forming an adherent oxide coating on it. This renders the metal passive. Were it not for this phenomenon we could not employ aluminium as a structural material since bare aluminium is highly reactive, $E^\circ(\mathrm{Al}^{3+}/\mathrm{Al})$ being -1.67 V.

8 Electroless Plating

The converse of metal dissolution is metal plating. Traditionally this has been carried out by making the object to be plated a cathode in a suitable plating bath, an operation that required appropriate electrical equipment. This is not necessary in so-called electroless plating where another couple is used to shift the potential sufficiently cathodic for metal deposition to occur. Once again we have two couples not in equilibrium. At the mixture potential there is a cathodic current due to the metal plating

$$\mathrm{M}^{n+} + ne^- \longrightarrow \mathrm{M(c)} \tag{25}$$

(where M could be Cu, Ni, or Au), and an anodic current – equal to it in magnitude – which flows by virtue of the electro-oxidation of a suitable reducing agent (like formaldehyde, hypophosphite, or borohydride). This mechanism was tested quantitatively by Paunovic.[16] He first determined the current–potential curve for the reduction of an alkaline solution of $\mathrm{Cu^{II}}$ complexed with EDTA at a copper foil electrode, and then the polarization curve for the oxidation of formaldehyde at the same pH at a similar copper electrode. The two curves were plotted on an Evans diagram where they intersected at the mixture potential (Figure 9). The current at E_{mix} corresponded, by Faraday's law, to a rate of copper formation of 2.2 mg $\mathrm{h^{-1}}$ $\mathrm{cm^{-2}}$ which agreed reasonably with the measured rate of copper deposition from the mixed solution of 1.8 ± 0.2 mg $\mathrm{h^{-1}}$ $\mathrm{cm^{-2}}$. Better agreement was obtained by another method[56] in which the rate of copper deposition, determined from low overpotential polarization data around the mixture potential, was 1.78 ± 0.20 mg $\mathrm{h^{-1}}$ $\mathrm{cm^{-2}}$ compared with the gravimetrically measured value of 1.59 mg $\mathrm{h^{-1}}$ $\mathrm{cm^{-2}}$.

Electroless deposition should not be confused with metal displacement (cementation) reactions. In the latter, the less noble metal (*e.g.*, iron) dissolves and gradually becomes coated with a more noble metal like copper. The process stops as soon as the iron surface is fully covered with a thin layer (< 1 μm) of copper.[57] In electroless deposition, however, the process can continue indefinitely. Indeed, since the deposited copper (say) acts as an electrode for the simultaneous anodic and cathodic processes, the deposition rate increases with the area of copper metal (equation 16) and so becomes autocatalytic. A striking visual example comes from an examination of old shipwrecks. Large grains of metallic copper have been found in some parts of sunken wooden vessels,[58] and these can be accounted for by

---

[56] M. Paunovic and D. Vitkavage, *J. Electrochem. Soc.*, 1979, **126**, 2282.

[57] H. O. Ali and I. R. A. Christie, *Gold Bull.*, 1984, **17**, 118.

[58] I. D. Macleod, *J. Electroanal. Chem.*, 1981, **118**, 291.

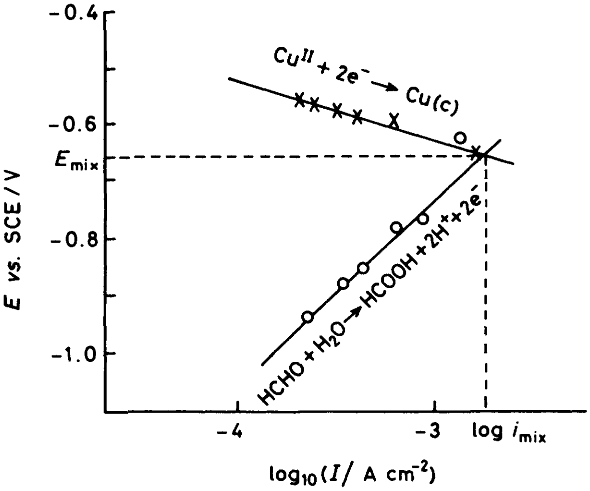

Figure 9 *Evans diagram for the electroless deposition of copper*

autocatalytic electroless deposition resulting from the reduction of copper ions (formed by the corrosion in seawater of copper, brass, and bronze articles) coupled with the oxidation of formaldehyde, one of the products of the slow degradation of cellulose in the wood.

The first practical application of electroless plating is attributed to Brenner and Riddell[59] in 1946 who immersed steel in an ammoniacal solution containing a nickel salt and hypophosphite. The reduction of the nickel was heterogeneously catalysed by the steel surface and further autocatalysed by the newly-formed nickel coating. Nickel plating is now often carried out this way on articles of various shapes, especially those of complex geometry. Similar plating processes have been developed for other metals, both singly and in combination,[60] particularly for the semiconductor industry.[61] Electroless plating is the preferred method for depositing metals on components that present electrically isolated islands, pads, and tracks.[57] These must first be mechanically roughened or chemically etched to improve the subsequent strength of metal adhesion. They are then activated with a preparation of colloidal palladium or gold which is easily reduced to a thin metal film that can initiate the electroless plating of the desired metal.[60] Metal oxides like α-PbO_2 or MnO_2 can also be deposited by electroless plating.[62] The contributory reactions here are the oxidation of the metal ion in a lower valence state (*e.g.*, Mn^{2+}) and the reduction of a strong oxidizing agent like $S_2O_8^{2-}$.

It is not often realized that the development of photographic plates depends

---

[59] A. Brenner and G. E. Riddell, *J. Res. Nat. Bur. Stand. U.S.*, 1946, **37**, 31.

[60] W. S. Rapson and T. Groenewald, *Gold Bull.*, 1975, **8**, 119.

[61] 'Science and Technology of Surface Coatings', ed. B. N. Chapman and J. C. Anderson, Academic Press, London, 1974.

[62] W. Mindt, *J. Electrochem. Soc.*, 1970, **117**, 615; 1971, **118**, 93.

upon another electroless autocatalytic plating process.[63] The essential component of a photographic film is silver halide. On its exposure to light some silver ions decompose at certain active centres to produce colloidal particles of metallic silver (the latent image). This must be intensified 10^8—10^9 times to form the visible photographic image by a process known as development. Various developing agents are known (*e.g.*, Fe^{2+}, hydroxylamine, hydroquinone, and their derivatives) but all are reducing agents which act by the basic equation

$$Ag^+ + \text{developer} \longrightarrow Ag(c) + \text{oxidized developer} \tag{26}$$

If this reaction occurred uniformly over the film one would only obtain a fogged plate. The true efficacy of reaction (26) depends on the fact that it proceeds by an electrochemical mechanism involving two current–potential curves. It can therefore come into operation only at the metallic silver sites of the latent image, and the latter grows autocatalytically until it becomes visible. At some well-judged point the developer must be removed, and after certain other operations the final picture is obtained.

9 Heterogeneous Catalysis of Redox Reactions

In metal dissolution, corrosion, and electroless plating the metal is itself a component of one of the interacting couples. We turn now to reactions between couples that take place at the surface of an independent metal or other electron-conducting solid.[64] A typical example is the redox reaction

$$2Fe(CN)_6^{3-} + 3I^- \longrightarrow 2Fe(CN)_6^{4-} + I_3^- \tag{27}$$

which is fairly slow in homogeneous aqueous solution but is catalysed by platinum, other noble metals,[65] and carbon.[66] The system can be qualitatively described by Figure 2, with curve 1 representing the anodic process

$$3I^- \longrightarrow I_3^- + 2e^- \tag{28}$$

and curve 2 the reduction

$$Fe(CN)_6^{3-} + e^- \longrightarrow Fe(CN)_6^{4-} \tag{29}$$

Quantitative proof of this interpretation has been obtained by a combination of electrochemical and kinetic experiments.[17,21] An anodically pre-conditioned platinum disk, rotated at 500 r.p.m., was first immersed in an iodide solution and the current–potential curve of half-reaction (28) was determined (curve I in Figure 10). After being cleaned and reconditioned, the disk was inserted into a

---

[63] W. Jaenicke, 'Electrochemical Aspects of the Photographic Processes', in 'Advances in Electrochemistry and Electrochemical Engineering', ed. H. Gerischer and C. W. Tobias, Wiley, New York, 1977, Vol. 10, p. 91.

[64] M. Spiro and A. B. Ravnö, *J. Chem. Soc.*, 1965, 78.

[65] M. Spiro, *J. Chem. Soc.*, 1960, 3678.

[66] J. M. Austin, T. Groenewald, and M. Spiro, *J. Chem. Soc.. Dalton Trans.*, 1980, 854.

hexacyanoferrate(III) solution so as to obtain the current–potential curve of half-reaction (29) (curve IIA in Figure 10). The two curves, with all currents taken as positive, intersect at a mixture potential of 0.551 V and a mixture current of 455($\pm$14) μA. In the third experiment, the disk was spun in a mixed solution of iodide and hexacyanoferrate(III). The disk adopted a potential of 0.552 V in the reaction mixture and the catalytic rate was found to be 4.96 ($\pm$0.06) $\times$ 10^{-9} mol s^{-1} which, by equation 15, corresponds to a current of 479 ($\pm$6) μA. This is shown as the ringed letter A in Figure 10. The mixture potential and current determined electrochemically are thus in close agreement with the corresponding properties derived from the independent catalytic run. These results, and similar ones obtained under other experimental conditions, clearly show that the catalysis of the $Fe(CN)_6^{3-}$ + I^- reaction proceeds by an electrochemical mechanism whereby electrons are transferred from I^- to $Fe(CN)_6^{3-}$ through the platinum metal. It may be added that the two ions need not occupy adjacent sites on the platinum surface, as would be the case for a Langmuir–Hinshelwood mechanism.

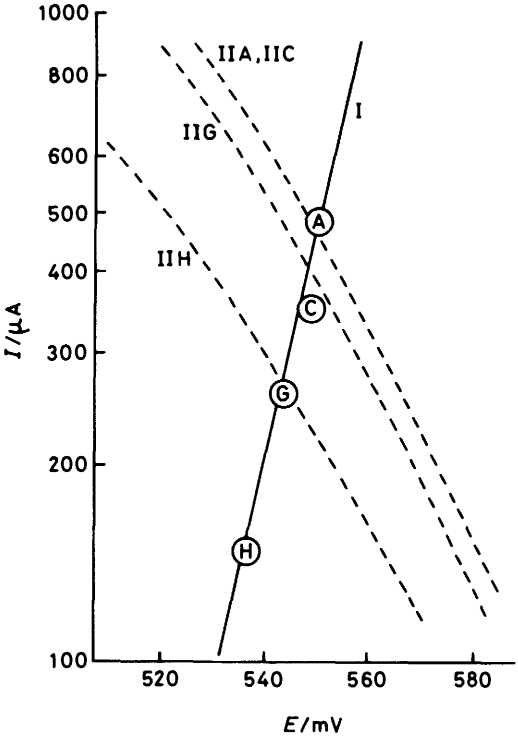

Figure 10 *Current–potential curves for iodide oxidation* (*curve* I) *and hexacyanoferrate*(III) *reduction* (*all curves labelled* II), *in* 1 mol dm^{-3} KNO_3 *at* 5 °C *at a platinum disk rotated at* 500 *r.p.m., after Spiro and Freund.*[21] *Letters A and C stand for anodic and cathodic pretreatments, respectively: letters G and H indicate cathodic pretreatment followed by exposure to iodide* (*see text*). *The ringed letters mark data obtained in the corresponding catalytic runs*

The electrochemical interpretation of redox catalysis explains many phenomena and allows us to make numerous predictions. Let us look at Figure 2 or 5(c). It is evident that if both curves rise steeply, *i.e.* if both couples are electrochemically reversible, the mixture currents will be large. Marked catalysis would therefore be expected for redox reactions between components of reversible couples. This has always been observed (apart from a few instances where the homogeneous redox reaction was so fast as to mask any heterogeneous effect).[64] Reactions involving the irreversible oxygen couple (equation 17) form another set that we can now understand. Because the i_0 value for the oxygen couple at platinum is only 10^{-10} A cm^{-2}, the slope of its current–potential curve is very small (*cf.* the cathodic curve in Figure 5(a) and the anodic curve in Figure 5(b)). Mixture currents will thus be tiny and little catalysis will be observed if the equilibrium potential of the other couple is close to that of the oxygen couple itself. The further away the Nernst potential of the other couple, and the more reversible it is (*i.e.* the steeper its I–E curve), the larger will be the mixture current and the more pronounced the catalysis by platinum. For example, Ce^{IV} can oxidize water to oxygen on a platinum surface in 2 mol dm^{-3} $HClO_4$ but not in 1 mol dm^{-3} H_2SO_4: this is consistent with the difference in the formal potentials of 0.47 V in the former medium and only 0.21 V in the latter (Table). It is also known that platinum catalyses the oxidation by oxygen of V^{III} to V^{IV} but no further oxidation to V^{V} takes place although such a process is thermodynamically feasible. The differences in the formal potentials of 0.89 V and 0.23 V, respectively, readily explain these observations in the light of the above discussion. There is clearly much scope for applying these ideas in inorganic and organic syntheses.

Table *Formal potentials of selected couples at* 25 °C[64]

Couple	*Medium*[a]	E^0/V
$\frac{1}{4}O_2 + H^+ + e^- \rightleftharpoons \frac{1}{2}H_2O$	1 M H_2SO_4	1.23
$Ce^{IV} + e^- \rightleftharpoons Ce^{III}$	2 M $HClO_4$	1.70
$Ce^{IV} + e^- \rightleftharpoons Ce^{III}$	1 M H_2SO_4	1.44
$V^{V} + e^- \rightleftharpoons V^{IV}$	1 M H_2SO_4	1.00
$V^{IV} + e^- \rightleftharpoons V^{III}$	1 M H_2SO_4	0.34

[a] M = mol dm^{-3}

Some surprising kinetic features were discovered by Woods[67] in studying another oxygen reaction, the platinum-catalysed oxidation of acetate ions

$$CH_3COO^- + H^+ + 2O_2 \longrightarrow 2CO_2 + 2H_2O \qquad (30)$$

He found that:

(*a*) With given oxygen and acetate concentrations, decrease of temperature from 94 °C to 50 °C hardly changed the catalytic rate although the potential taken up

---

[67] R. Woods, *J. Catal.*, 1970, **16**, 267.

by the platinum catalyst increased from 0.28 V to 0.45 V. At 40 °C the potential suddenly jumped to 1.05 V and the catalytic activity decreased by two orders of magnitude.

(*b*) At a given temperature and acetate concentration, the rate of the catalysed reaction increased linearly with the concentration of oxygen up to a certain critical value. Above this value the catalytic rate dropped by two orders of magnitude.

Woods showed that these intriguing results can easily be understood in electrochemical terms. The current–potential curves for the half-reaction

$$CH_3COO^- + 2H_2O \longrightarrow 2CO_2 + 7H^+ + 8e^- \qquad (31)$$

in deoxygenated solution are drawn in Figure 11, as is the dotted curve for the reduction of O_2 in oxygen-saturated solution with the current taken as positive. The limiting oxygen current density varied little with temperature so that the mixture currents – the currents at which the curves cross –were almost temperature independent. The mixture potentials can be seen to increase as the temperature falls. The acetate curve at 40 °C, however, lies below the oxygen limiting current and so the two curves can only intersect at the much higher potential of 1.05 V where the oxygen current is almost zero. Now consider the 40 °C situation again. At low oxygen concentrations, where the oxygen limiting current is proportionately smaller (equation 14), the acetate curve crosses the oxygen curve in the limiting

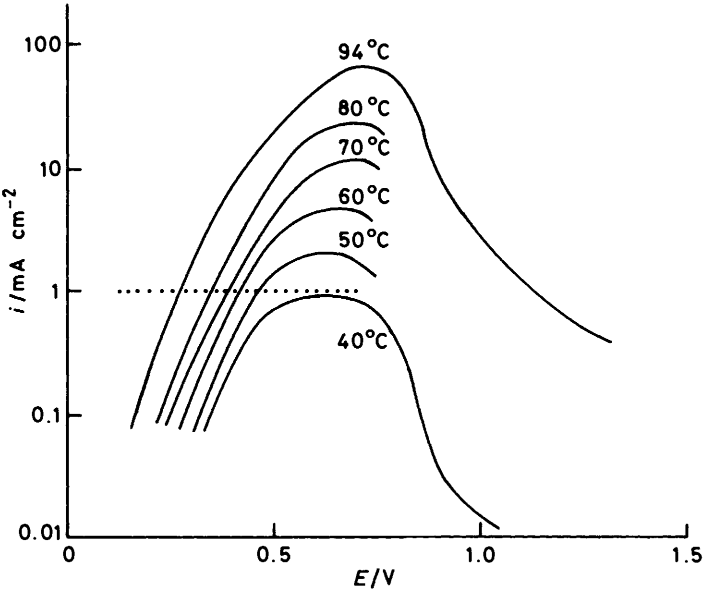

Figure 11 *Current–potential curves for the oxidation of acetate in deoxygenated solutions at various temperatures (full curves) and for the reduction of oxygen (dotted curve), after Woods*[67]

current region. The larger the oxygen concentration, the greater the limiting and mixture currents and therefore the greater the catalytic rate. But as soon as the oxygen concentration is large enough for its limiting current to exceed the maximum acetate current, a sudden increase in the mixture potential and a concomitant drop in mixture current must set in as the crossing point of the curves shifts abruptly. Phenomena (*a*) and (*b*) are thus seen to be natural outcomes of the electrochemical mechanism of the catalysis. As a further test of this mechanism, Woods measured the amount of CO_2 produced in an oxygenated acetate solution at 80 °C. The experimental value of 0.26 mg min^{-1} agreed well with that of 0.28 mg min^{-1} calculated by Faraday's law from the oxygen reduction current.

Woods[68] also investigated an important catalytic reaction that makes certain kinds of froth flotation possible. Froth flotation is used to separate minerals such as galena (PbS, a major source of the world's lead supplies) from sand and other worthless 'gangue' materials. The ore is ground up and mixed with water and a 'collector' such as potassium ethyl xanthate, $EtOCS_2^-K^+$. When a stream of air bubbles is passed through, the galena particles attach themselves to the bubbles and rise as a froth while the gangue remains wetted below. The froth is removed from the surface and collapsed, and the galena is recovered from it. The process works only because the xanthate has rendered the galena particles hydrophobic. It has now been established that the hydrophobic layer is actually adsorbed dixanthogen. Its formation requires the presence of oxygen to allow the following simultaneous electrochemical processes to take place on the semiconducting galena surface:

$$2EtOCS_2^- \longrightarrow (EtOCS_2)_2 + 2e^- \qquad (32)$$

$$\tfrac{1}{2}O_2 + H_2O + 2e^- \longrightarrow 2OH^- \qquad (33)$$

Galena and other flotable sulphide minerals are known to catalyse the reaction between oxygen and xanthates to form dixanthogen. Xanthate is also an efficient collector for native metals like copper and gold and these would certainly be expected to catalyse the reaction. However, xanthate is unable to collect silicates and oxides, probably because their non-conducting surfaces cannot sustain the electrochemical mechanism.

During the last few years the kinetic consequences of the electrochemical mechanism have been developed further. Special attention has been paid to two types of joint control (*cf.* Figure 5(c)). In the first, the current–potential curves are very steep because both couples are highly reversible. Their high exchange current densities lead to an extremely fast interaction between the couples on the surface, so fast that the chemical reaction on the catalyst surface effectively comes to equilibrium. The bulk reaction mixture approaches equilibrium more slowly, the rate-determining steps being diffusion of species to and from the surface. A mathematical analysis of this situation[33] gives a value for i_{mix} and hence, by equation 16, for the catalytic rate V. The equation predicted for the $Fe(CN)_6^{3-}$ + I^- reaction (27) is

---

[68] R. Woods, *J. Phys. Chem.*, 1971, **75**, 354.

$$V = k'f^{1/2}[\mathrm{Fe(CN)_6}^{3-}]^{2/3}[\mathrm{I}^-] \tag{34}$$

if the reaction takes place at a catalytic platinum disk rotating at a frequency f. Both the frequency dependence and the kinetic orders were confirmed in an experimental study.[69] It was also found that the activation energy associated with k' was negative, -16.9 kJ mol^{-1}, an unusual result but one that was in close agreement with the theoretical prediction of -17.1 kJ mol^{-1}.

The second type of joint control that is being explored in more detail concerns two couples of intermediate or low reversibility. If the current–potential curves in Figure 5(c) are both in their respective Tafel regions at E_{mix}, then equation 13(a) can be applied to one couple and equation 13(b) to the other. The two current densities i are now equal to i_{mix}. Introducing equations 2, 9, 18, and 16 leads to a kinetic equation for the catalytic rate.[31] This has recently been tested[70] for the reaction

$$\mathrm{Fe(CN)_6}^{3-} + \mathrm{S_2O_3}^{2-} \longrightarrow \mathrm{Fe(CN)_6}^{4-} + \tfrac{1}{2}\mathrm{S_4O_6}^{2-} \tag{35}$$

catalysed by a citrate-stabilized gold sol. A colloidal catalyst was chosen because the diffusion layer thickness at small particles is very small: diffusion to and from the surface is therefore fast and the catalysed reaction becomes completely surface-controlled. For reaction 35 the theory predicted that

$$V = k''[\mathrm{Fe(CN)_6}^{3-}]^{r_1}[\mathrm{S_2O_3}^{2-}]^{r_2} \tag{36}$$

where the kinetic orders r_1 and r_2 are unequal fractions that should add up to unity. The experimental results of $r_1 = 0.53 \pm 0.03$ and $r_2 = 0.42 \pm 0.03$ closely met these requirements. The catalytic kinetics for these two different types of redox reaction have therefore been successfully predicted by the electrochemical model.

10 The Validity of the Additivity Hypothesis

The additivity hypothesis postulates that the current–potential curve of a mixture of couples can be obtained simply by adding the current–potential curves of the separate couples. Much direct and circumstantial evidence has accumulated to support this attractive idea. Several tests of the additivity hypothesis have been mentioned in this review. Despite its widespread success, however, several cases have recently come to light that throw doubt on the universal applicability of the hypothesis. Let us look at the evidence.

Figure 10 shows how well the additivity hypothesis fits the catalytic results for the $\mathrm{Fe(CN)_6}^{3-} + \mathrm{I}^-$ reaction (27) on an anodically preconditioned platinum surface. On a cathodically pretreated platinum surface, however, the agreement was much poorer.[21] Although the current–potential curve of the iodide couple (curve I) and of the ferricyanide couple (curve IIC) were unaffected by this change in pretreatment, their intersection point can be seen to be appreciably higher than the ringed point C which represents the rate and potential of the catalytic run carried out in the mixed solution. This suggests interference between the couples when they

---

[69] P. L. Freund and M. Spiro, *J. Chem. Soc.. Faraday Trans. 1*, 1983, **79**, 491.

[70] P. L. Freund and M. Spiro, *J. Chem. Soc.. Faraday Trans. 1*, 1986, **82**, in press.

are present together at a reduced platinum surface. Since iodide ions do not adsorb on anodically preconditioned platinum but do show specific adsorption on the cathodically preconditioned metal, it seems likely that adsorbed iodide ions are blocking the surface for ferricyanide reduction. This explanation is strongly supported by further experiments. The *I–E* curve for ferricyanide reduction (curve IIG) was itself lowered when a cathodically pretreated electrode was used that had been immersed for 10 min in a KI solution and then well rinsed. The curve was lower still (curve IIH) if the electrode, before being rinsed, had been exposed to a 4-hour-old $Fe(CN)_6^{3-} + I^-$ mixture which contained both iodide ions and iodine. The respective catalytic rates (ringed G and ringed H) were even smaller. It is noteworthy that all these catalytic points lie on the iodide current–potential curve I (which was unaffected by the different conditioning methods). This demonstrates that the catalysis of the $Fe(CN)_6^{3-} + I^-$ reaction still proceeds by electron transfer through the platinum even though the ferricyanide reduction is being hindered by adsorbed iodide and iodine species.

Other redox reactions involving iodide ions in the presence of reduced platinum surfaces should show similar effects. A case that has recently been discovered in our laboratory is the oxidation of I^- ions by molecular dioxygen. This reaction was not catalysed by platinum although a sizeable mixture current is predicted from the current–potential curves of the two separate couples.[71] Departures from additivity may therefore be anticipated whenever one of the couples (or both) contains strongly adsorbing species. An example is provided by the thionine/leucothionine and Fe^{3+}/Fe^{2+} couples. When a platinum electrode is immersed in a dilute thionine solution it becomes covered with a monolayer of adsorbed dye whose presence decreases the electrochemical rate constant $k^{\ominus}$ of the Fe^{3+}/Fe^{2+} couple by a factor of *ca.* 5.[72] If the electrode is anodically precoated with some 20 monolayers of thionine, $k^{\ominus}$ for the iron couple is reduced 100-fold while the thionine couple itself remains fairly reversible.[73] This makes a thionine-coated electrode suitable as the illuminated electrode in a photogalvanic cell, and illustrates that departures from the simple additivity hypothesis can also be put to good use.

An interesting example comes from a study of electroless gold plating. With an alkaline plating bath containing $Au(CN)_2^-$ and BH_4^-, Okinaka[74] found that the deposition rate passed through a maximum as the $Au(CN)_2^-$ concentration increased. This could be accounted for by competitive adsorption on the gold surface between the strongly adsorbing $Au(CN)_2^-$ ions and BH_3OH^-, the active reducing agent formed by hydrolysis of BH_4^-. Competitive adsorption can also explain the observation that, in the catalysis by a platinum sol of the oxidation of formic acid by methylene blue, the rate *decreased* with increasing concentration of methylene blue.[75] The strong adsorption of this dye and its reduction product on platinum electrodes has recently been investigated.[76] Phenomena of this kind are of

---

[71] A. M. Creeth and M. Spiro, unpublished work.

[72] M. D. Archer, M. I. C. Ferreira, W. J. Albery, and A. R. Hillman, *J. Electroanal. Chem.*, 1980, **111**, 295.

[73] W. J. Albery, W. R. Bowen, F. S. Fisher, A. W. Foulds, K. J. Hall, A. R. Hillman, R. G. Egdell, and A. F. Orchard, *J. Electroanal. Chem.*, 1980, **107**, 37.

course well known in the heterogeneous catalysis of gas reactions.[77] Here the literature contains numerous examples in which one reactant or a product 'poisons' a catalyst by occupying too many sites on the surface. In retrospect, it may seem remarkable that so few instances of mutual interference have been reported in the field of mixed couples. Three reasons for this can be suggested. First, the ubiquitous presence of solvent means that any species must compete with solvent molecules for surface sites; fewer species therefore adsorb at all and the majority of molecules that adsorb from dilute solution form no more than a monolayer.[78] Second, many of the processes in question are diffusion controlled, and under such conditions the surface concentration of one of the reactants may approach zero and so cause negligible interference to the other reactant.[67] Lastly, it should not be forgotten that in metal dissolution and in certain corrosion processes a fresh surface is continually forming and thereby removing adsorbed material. In all cases, however, one needs to distinguish carefully between species that are reversibly adsorbed and those (like I^- on cathodically pretreated platinum) that are adsorbed irreversibly.

11 Conclusion

The previous section has dealt with a few situations in which the current–potential curves of the separate couples cannot be treated additively when the couples are present together. In most cases the currents at a given potential *can* be added up, at least to a good first approximation. As the present review has shown, this simple treatment very satisfactorily explains a great variety of chemical phenomena ranging from the poisoning of electrodes, the dissolution of metals (whether desirable as in mineral extraction or undesirable as in corrosion), the electroless deposition of metals in industry and in photographic development, and the heterogeneous catalysis by metals of a wide range of redox reactions.

Acknowledgement. I am grateful to Professor A. K. Covington and to Mr. A. M. Creeth for constructive comments on the original manuscript.

---

[74] Y. Okinaka, *J. Electrochem. Soc.*, 1973, **120**, 739.

[75] H. v. Euler and A. Ölander, *Z. Physik. Chem.*, 1928, **137A**, 29.

[76] V. Svetlicic, V. Zutic, J. Clavilier, and J. Chevalet, *J. Electroanal. Chem.*, 1985, **195**, 307.

[77] R. P. H. Gasser, 'An Introduction to Chemisorption and Catalysis by Metals', Oxford University Press, 1985, Chapt. 8.

[78] G. D. Parfitt and C. H. Rochester, 'Adsorption of Small Molecules', in 'Adsorption from Solution at the Solid/Liquid Interface', ed. G. D. Parfitt and C. H. Rochester, Academic Press, London, 1983, Chapt. 1.